

Spontaneous CP violation in $A_4 \times SU(5)$ with constrained sequential dominance 2Stefan Antusch,^{1,*} Stephen F. King,^{2,†} and Martin Spinrath^{3,‡}¹*Department of Physics, University of Basel, Klingelbergstrasse 82, CH-4056 Basel, Switzerland and Max-Planck-Institut für Physik (Werner-Heisenberg-Institut), Föhringer Ring 6, D-80805 München, Germany*²*School of Physics and Astronomy, University of Southampton, SO17 1BJ Southampton, United Kingdom*³*SISSA/ISAS and INFN, Via Bonomea 265, I-34136 Trieste, Italy*

(Received 5 March 2013; published 28 May 2013)

We revisit a two right-handed neutrino model with two texture zeros, namely an indirect model based on A_4 with the recently proposed new type of constrained sequential dominance (CSD2), involving vacuum alignments along the $(0, 1, -1)^T$ and $(1, 0, 2)^T$ directions in flavor space, which are proportional to the neutrino Dirac mass matrix columns. In this paper we construct a renormalizable and unified indirect $A_4 \times SU(5)$ model along these lines and show that, with spontaneous CP violation and a suitable vacuum alignment of the phases, the charged lepton corrections lead to a reactor angle in good agreement with results from Daya Bay and RENO. The model predicts a right-angled unitarity triangle in the quark sector and a Dirac CP violating oscillation phase in the lepton sector of $\delta \approx 130^\circ$, while providing a good fit to all quark and lepton masses and mixing angles.

DOI: [10.1103/PhysRevD.87.096018](https://doi.org/10.1103/PhysRevD.87.096018)

PACS numbers: 11.30.Hv, 12.10.-g, 12.15.Ff, 14.60.Pq

I. INTRODUCTION

The lepton mixing angles have the distinctive feature that the atmospheric angle θ_{23} and the solar angle θ_{12} , are both rather large [1]. Direct evidence for the reactor angle

θ_{13} was first provided by T2K, MINOS, and Double Chooz [2–4]. Subsequently Daya Bay [5], RENO [6], and Double Chooz [7] Collaborations have measured $\sin^2(2\theta_{13})$,

$$\begin{aligned} \text{Daya Bay:} & \quad \sin^2(2\theta_{13}) = 0.089 \pm 0.011(\text{stat}) \pm 0.005(\text{syst}), \\ \text{RENO:} & \quad \sin^2(2\theta_{13}) = 0.113 \pm 0.013(\text{stat}) \pm 0.019(\text{syst}), \\ \text{Double Chooz:} & \quad \sin^2(2\theta_{13}) = 0.109 \pm 0.030(\text{stat}) \pm 0.025(\text{syst}). \end{aligned} \tag{1.1}$$

This rules out the hypothesis of exact tri-bimaximal (TB) mixing [8], and many alternative proposals have recently been put forward [9], although there are relatively few examples which also include unification [10–13]. For example, an attractive scheme based on trimaximal (TM) mixing remains viable [14], sometimes referred to as TM_2 mixing since it maintains the second column of the TB mixing matrix and hence preserves the solar mixing angle prediction $\sin \theta_{12} \approx 1/\sqrt{3}$. However there is another variation of TM mixing which also preserves this good solar mixing angle prediction by maintaining the first column of the TB matrix, namely TM_1 mixing [15].

Although there were models of TM_2 mixing which can account for the smallness of the reactor angle [16], the first model in the literature for TM_1 mixing, which also fixed the value of the reactor angle, was proposed in [17]. The model discussed in [17] was actually representative of a general strategy for obtaining TM_1 mixing using sequential dominance (SD) [18] and vacuum alignment. The strategy of combining SD with vacuum alignment is familiar from the constrained sequential dominance (CSD) approach to

TB mixing [19] where a neutrino mass hierarchy is assumed and the dominant and subdominant flavons responsible for the atmospheric and solar neutrino masses are aligned in the directions of the third and second columns of the TB mixing matrix, namely $\langle \phi_1^v \rangle \propto (0, 1, -1)^T$ and $\langle \phi_2^v \rangle \propto (1, 1, 1)^T$. The new idea was to maintain the usual vacuum alignment for the dominant flavon, $\langle \phi_1^v \rangle \propto (0, 1, -1)^T$ as in CSD, but to replace the effect of the subdominant flavon vacuum alignment by a different one, namely either $\langle \phi_{120} \rangle \propto (1, 2, 0)^T$ or $\langle \phi_{102} \rangle \propto (1, 0, 2)^T$, where such alignments may be naturally achieved from the standard ones using orthogonality arguments.

We referred to this new approach as CSD2¹ and showed that it leads to TM_1 mixing and a reactor angle which, at leading order, is predicted to be proportional to the ratio of the solar to the atmospheric neutrino masses, $\theta_{13} = \frac{\sqrt{2}}{3} \frac{m_2^v}{m_3^v}$.

¹It is interesting to compare the predictions of CSD2 to another alternative to CSD that has been proposed to account for a reactor angle called partially constrained sequential dominance (PCSD) [20]. PCSD involves a vacuum misalignment of the dominant flavon alignment to $(\epsilon, 1, -1)^T$, with a subdominant flavon alignment $(1, 1, 1)^T$, leading to tri-bimaximal-reactor mixing [20] in which only the reactor angle is switched on, while the atmospheric and solar angles retain their TB values.

*stefan.antusch@unibas.ch

†king@soton.ac.uk

‡spinrath@sisssa.it

The model was proposed before the results from Daya Bay and RENO, and the prediction turned out to be rather too small compared to the results in Eq. (1.1). More generally it has been shown that any type I seesaw model with two right-handed neutrinos and two texture zeros in the neutrino Yukawa matrix (as in Occam’s razor) is not compatible with the experimental data for the case of a normal neutrino mass hierarchy [21]. However this conclusion ignores the effect of charged lepton corrections, and so an “Occam’s razor” model which includes such corrections may become viable.

In the present paper we construct a fully renormalizable unified $A_4 \times SU(5)$ model in which the neutrino sector satisfies the CSD2 conditions, and show that, with spontaneous CP violation and a suitable vacuum alignment of the phases, the charged lepton corrections can correct the reactor angle, bringing it into agreement with results from Daya Bay and RENO. We shall use here similar techniques as in [22], where spontaneous CP violation with flavon phases determined by the vacuum alignment was discussed for the first time, in order to ensure that the charged lepton mixing angle correction (typically about $\sim 3^\circ$) adds constructively to the θ_{13}^{ν} angle from the neutrino sector (typically about $\sim 5^\circ\text{--}6^\circ$) leading to $\theta_{13} \sim 8^\circ\text{--}9^\circ$, within the range of the measured value from Daya Bay and RENO. In fact the present model is more ambitious, since it describes all quark and lepton masses and mixing angles, including predictions for all the CP violating phases.

We demonstrate the viability of the model by performing a global fit to the charged lepton masses and the quark masses and mixing parameters. For the neutrino mixing angles we make a parameter scan and find very good agreement with the experimental data. We emphasize that the present $A_4 \times SU(5)$ model represents one of the first unified “indirect” family symmetry models in the literature that has been constructed to date that is consistent with all experimental data on quark and lepton mass and mixing parameters where indirect simply means that the family symmetry is completely broken by the vacuum alignment.² For a review see [23].

We emphasize that the idea of spontaneous CP violation has a long history [24]. However, in explicit flavor models using this idea only the positions of the phases in the mass matrices was predicted, but not the phases of the flavon fields themselves (see, e.g., [25]). Spontaneous CP violation with calculable flavon phases from vacuum alignment was first discussed in [22] and demonstrated in example models based on A_4 and S_4 . In this paper we shall use a similar approach where the A_4 model is formulated in the real $SO(3)$ basis (see, e.g., [26]) and where we only consider the real representations **1** and **3**. In such a framework, one

²In fact the only other example of a unified indirect model with a realistic reactor angle that we are aware of is the last paper in [12] based on Pati-Salam unification, however that model predicts an atmospheric angle in second octant.

can either use a “simple” CP symmetry under which the components of the scalar fields transform trivially as $\phi_i \rightarrow \phi_i^*$, or a “generalized” CP symmetry which intertwines CP with A_4 (see, e.g., [27] and references therein). In the latter case, in our basis, the triplet fields would transform as $\phi_i \rightarrow U_3 \phi_i^*$, where U_3 interchanges the second and third component. When complex **1'** and **1''** representations are used in a model, the U_3 transformation then takes care of the fact that under CP the two complex singlets are interchanged with each other. However, as already mentioned above, in our model this will make no difference. CP symmetry leads to real coupling constants in a suitable field basis (after “unphysical” phases have been absorbed by field redefinitions). CP is subsequently spontaneously broken by the flavon vacuum alignment, which is controlled by additional Abelian symmetries \mathbb{Z}_3 and \mathbb{Z}_4 , resulting in calculable complex flavon phases as in [22].

The layout of the rest of the paper is as follows: In the next section we discuss the general strategy we will adopt in our model. After a brief review of CSD2 we discuss charged lepton sector corrections to TM_1 mixing before we describe the method which we use to fix the flavon value expectation values (VEVs). In Sec. III we describe our model, the field content and symmetries and the resulting Yukawa and mass matrices. The justification for the chosen vacuum alignment including phases is given in Sec. IV. In the subsequent sections we comment on the Higgs mass and then we give the numerical results from our global fit and scans. In Sec. VII we summarize and conclude and in the Appendixes we define our notations and conventions and give the messenger sector of our model.

II. THE STRATEGY

Let us now describe our general idea in somewhat more detail, before we present an explicit GUT model example in the next section. As outlined in the introduction, we are combining three ingredients which finally result in a highly predictive unified flavor model. These ingredients are:

- (i) CSD2 for the neutrino mixing angles θ_{ij}^{ν} ,
- (ii) charged lepton mixing contributions as they are typical in GUTs,
- (iii) spontaneous CP violation with aligned phases.

We now briefly describe these three concepts and the resulting new class of models.

A. CSD2 in the neutrino sector

In models with CSD2 [17], the neutrino mass matrix is dominated by two right-handed neutrinos with mass matrix $M_R = \text{diag}(M_A, M_B)$ and couplings to the lepton doublets $A = (0, a, -a)^T$ and $B = (b, 0, 2b)^{T3}$ such that the neutrino Yukawa matrix takes the form $Y_\nu = (A, B)$, in

³ $B = (b, 2b, 0)^T$ was also considered in [17], but here we shall not consider it further.

left-right convention. A summary of the used conventions is given in the Appendix A.

After the seesaw mechanism is implemented, CSD2 leads to the following light effective neutrino Majorana mass matrix:

$$M_\nu = m_a \begin{pmatrix} 0 & 0 & 0 \\ 0 & 1 & -1 \\ 0 & -1 & 1 \end{pmatrix} + m_b \begin{pmatrix} 1 & 0 & 2 \\ 0 & 0 & 0 \\ 2 & 0 & 4 \end{pmatrix} \\ = m_a \begin{pmatrix} \epsilon e^{i\alpha} & 0 & 2\epsilon e^{i\alpha} \\ 0 & 1 & -1 \\ 2\epsilon e^{i\alpha} & -1 & 1 + 4\epsilon e^{i\alpha} \end{pmatrix}, \quad (2.1)$$

where $m_a = \frac{v_a^2 a^2}{M_A}$, $m_b = \frac{v_b^2 b^2}{M_B}$, and where α is the relative phase difference between m_a and m_b . We define $\epsilon = |m_b|/|m_a|$, and assume $\epsilon \ll 1$ leading to a normal mass hierarchy in accordance with SD. As discussed in Appendix A we use here different conventions than in the original CSD2 paper [17] which are more convenient in the context of $SU(5)$ GUTs.

Only three parameters, e.g., m_a , ϵ , and α , govern the neutrino masses and mixing parameters. For the mixing parameters, the predicted values are, to leading order in ϵ (from [17] with adapted conventions⁴),

$$s_{23}^\nu \approx \frac{1}{\sqrt{2}} - \frac{\epsilon}{\sqrt{2}} \cos \alpha, \quad \delta_{13}^\nu \approx \pi - \alpha + \epsilon \frac{5}{2} \sin \alpha, \quad (2.2)$$

$$s_{13}^\nu \approx \frac{\epsilon}{\sqrt{2}}, \quad \alpha_2 \approx -\alpha + 2\epsilon \sin \alpha, \quad (2.3)$$

$$s_{12}^\nu \approx \frac{1}{\sqrt{3}}. \quad (2.4)$$

The mixing scheme resulting from CSD2 can be identified as trimaximal mixing of type 1 (i.e., TM_1 [15]) but with a predicted value of the neutrino 1–3 mixing, $\theta_{13}^\nu = \frac{\sqrt{2}}{3} \frac{m_2^\nu}{m_3^\nu} \sim 5^\circ - 6^\circ$. With neutrino mass $m_1^\nu = 0$, only one Majorana CP phase is physical. Without charged lepton corrections, δ_{13}^ν would be identical with the leptonic Dirac CP phase δ . Let us also note that CSD2 predicts a deviation of θ_{23}^ν from 45° , depending on the phase α .

B. Charged lepton mixing contribution in GUTs

In GUT models the charged lepton Yukawa matrix is generically nondiagonal in the flavor basis, due to the close link between the charged lepton and the down-type quark Yukawa matrices, which typically provides the main origin of the flavor mixing in the quark sector. With the Cabibbo angle θ_C being the largest mixing in the quark sector, the mixing in Y_e is often dominated by a 1–2 mixing θ_{12}^e as

well, such that the relevant part of (the hierarchical matrix) Y_e can be written as

$$Y_e \approx \begin{pmatrix} 0 & ce^{i\beta} & 0 \\ * & d & 0 \\ 0 & * & * \end{pmatrix}, \quad (2.5)$$

where c , d , and β are real and where the entries marked by a “*” are not relevant for our discussion here. With $c \ll d$ one can read off to leading order the values for the complex 1–2 mixing angle (for more details see also Appendix A) that are

$$\theta_{12}^e \approx \left| \frac{c}{d} \right| \quad \text{and} \quad \delta_{12}^e = \begin{cases} -\beta & \text{for } c/d > 0 \\ -\beta + \pi & \text{for } c/d < 0 \end{cases}. \quad (2.6)$$

Since we will have $c/d < 0$ in our example GUT model in the next section, let us consider this case also in the following discussion.

In explicit GUT models, θ_{12}^e is typically related to the Cabibbo angle by group theoretical Clebsch factors from GUT breaking, as has been discussed recently, e.g., in [10,11]. In many GUT models, in particular in those where the muon and the strange quark mass at the GUT scale is predicted by such a Clebsch factor as $m_\mu/m_s = 3$ [28], but also if the Yukawa matrices Y_e (and Y_d) are (nearly) symmetric with a zero in the (0,0) element [10], θ_{12}^e is predicted as

$$\theta_{12}^e \approx \frac{\theta_C}{3}. \quad (2.7)$$

In the example GUT model in the next section we will see explicitly how such a prediction arises in an $SU(5)$ GUT.

The leptonic mixing parameters, defined via $U_{\text{PMNS}} = U_e U_\nu^\dagger$, are a combination of the mixing from the neutrino and the charged lepton sectors. Making use of the fact that, to leading order, $\theta_{23}^e = \theta_{13}^e = \delta_{12}^\nu = \delta_{23}^\nu = 0$, and using the CSD2 expressions from above for the neutrino sector, and general formulas for the charged lepton mixing contributions of [19,29,30]

$$s_{23} e^{-i\delta_{23}} = s_{23}^\nu e^{-i\delta_{23}^\nu} - \theta_{23}^e c_{23}^\nu e^{-i\delta_{23}^e}, \quad (2.8)$$

$$s_{13} e^{-i\delta_{13}} = \theta_{13}^\nu e^{-i\delta_{13}^\nu} - \theta_{12}^e s_{23}^\nu e^{-i(\delta_{23}^\nu + \delta_{12}^e)}, \quad (2.9)$$

$$s_{12} e^{-i\delta_{12}} = s_{12}^\nu e^{-i\delta_{12}^\nu} - \theta_{12}^e c_{23}^\nu c_{12}^\nu e^{-i\delta_{12}^e}, \quad (2.10)$$

we obtain [up to $\mathcal{O}(\epsilon)$]

$$\theta_{23} \approx 45^\circ - \epsilon \cos \alpha, \quad (2.11)$$

$$\theta_{13} \approx \frac{\epsilon}{\sqrt{2}} - \cos(\beta - \alpha) \frac{\theta_{12}^e}{\sqrt{2}}, \quad (2.12)$$

$$\theta_{12} \approx 35.3^\circ + \cos \beta \frac{\theta_{12}^e}{\sqrt{2}}, \quad (2.13)$$

⁴Compared to the notation of [17], we have changed, for instance, $\alpha \rightarrow -\alpha$.

where $\epsilon \approx \frac{2}{3} \frac{m_s^2}{m_3^2} \approx 8.4^\circ$. When the phases α and β are fixed by the vacuum alignment, and when also θ_{12}^e is predicted from the GUT structure, as both will be the case in our model, all three mixing angles and also the CP phases δ and α_2 , are predicted. Thus, the resulting models of this type can be highly predictive.

We would like to note here already that in the explicit GUT model in the next section, we will construct a vacuum alignment such that $\alpha = \pi/3$, leading to⁵

$$\theta_{23} \approx 45^\circ - \frac{\epsilon}{2} \approx 41^\circ, \quad (2.14)$$

close to the best fit value for the normal hierarchy case from global fits to the neutrino data [31]. The alignment of β will satisfy $\beta = \alpha + \pi$, such that the neutrino and charged lepton contributions to θ_{13} simply add up, leading to (with $\theta_{12}^e = \theta_C/3$)

$$\theta_{13} \approx \frac{\epsilon}{\sqrt{2}} + \frac{\theta_C}{3\sqrt{2}} \approx 8^\circ - 9^\circ, \quad (2.15)$$

in agreement with the recent measurements. With these values of α and β , it also turns out that θ_{12} is predicted somewhat smaller than 35° , namely

$$\theta_{12} \sim 33^\circ. \quad (2.16)$$

This value of θ_{12} could be distinguished from the tri-bimaximal value by a future reactor experiment with ~ 60 km baseline [32].

C. Spontaneous CP violation with aligned phases

Finally, the third ingredient is spontaneous CP violation with aligned phases of the flavon VEVs, using the method proposed in [22]. To give a brief summary of this method, let us note that phase alignment can very simply be achieved using discrete symmetries when the flavon VEVs effectively depend on one parameter, i.e., when the direction of the VEVs is given by the form of the potential. This remains true even in the presence of generalized CP transformations as long as these CP transformations fix the phases of the involved coupling constants. Working example models with A_4 and S_4 family symmetry can be found in [22]. Note that S_4 is in agreement only with simple CP , while the generalized CP transformation for A_4 interchanges the complex singlet representations [27]. In both cases all the coupling constants are forced to be real in a suitable field basis.

To illustrate the phase alignment, let us consider a case with a flavon field ξ which is a singlet under the family

⁵We note that the choice $\alpha = \pi/3$ is motivated by the current data which favours θ_{23} in the first octant. On the other hand, one can in principle also construct other models with different values of α , and there are also other options for β and θ_{12}^e , which may lead to interesting alternative models. In this sense, the strategy described here leads to a whole new class of possible models.

symmetry and singly charged under a \mathbb{Z}_n shaping symmetry (with $n \geq 2$). Then typical terms in the flavon superpotential, which “drive” the flavon VEV nonzero, have the form

$$P \left(\frac{\xi^n}{\Lambda^{n-2}} \mp M^2 \right). \quad (2.17)$$

The field P is the so-called “driving superfield,” meaning that the F -term $|F_P|^2$ generates the potential for ξ which enforces a nonzero VEV. Λ is the (real and positive) suppression scale of the effective operator, and M here is simply a (real) mass scale. From the potential for ξ ,

$$|F_P|^2 = \left| \frac{\xi^n}{\Lambda^{n-2}} \mp M^2 \right|^2, \quad (2.18)$$

the VEV of ξ has to satisfy

$$\xi^n = \pm \Lambda^{n-2} M^2. \quad (2.19)$$

Since the right side of the equation is real, we obtain that

$$\arg(\langle \xi \rangle) = \begin{cases} \frac{2\pi}{n} q, & q = 1, \dots, n & \text{for “-” in Eq. (2.17)} \\ \frac{2\pi}{n} q + \frac{\pi}{n}, & q = 1, \dots, n & \text{for “+” in Eq. (2.17)} \end{cases}. \quad (2.20)$$

For example, with a \mathbb{Z}_3 shaping symmetry and a + in Eq. (2.17), only multiples of $\pi/3$ are allowed for $\arg(\langle \xi \rangle)$. We will use this method for the relevant flavons to constrain their phases. In the ground state, one of the vacua (with a fixed phase) is selected, which finally determines also the two phases α and β relevant for the predictions in the lepton sector.

Furthermore, we note that we will also use the phase alignment to generate the CP violation in the quark sector, predicting a right-angled unitarity triangle, which is in excellent agreement with the present data (making use of the quark phase sum rule from [33]).

We now turn to an explicit GUT model, where the above described strategy is applied.

III. THE MODEL

In the following we will construct an $A_4 \times SU(5)$ model with CSD2 [17] in the neutrino sector. The model follows the strategy described in the previous section, such that the charged lepton mixing contribution to θ_{13} adds up constructively with the 1–3 mixing in the neutrino sector to $\theta_{13} \sim 8^\circ - 9^\circ$, with the phases fixed by the “discrete vacuum alignment” mechanism [22].

The matter and the Higgs sector of the model is summarized in Table I while the required flavons are shown in Table II. The superpotential after integrating out the heavy messenger fields (see Appendix B) and suppressing order one coefficients read

$$\mathcal{W}_N = \xi_1 N_1^2 + \xi_2 N_2^2, \quad (3.1)$$

TABLE I. The matter and Higgs fields in our model and their quantum numbers.

	T_1	T_2	T_3	F	N_1	N_2	H_5	\bar{H}_5	H_{45}	\bar{H}_{45}	H_{24}	S
$SU(5)$	10	10	10	$\bar{5}$	1	1	5	$\bar{5}$	45	$\bar{45}$	24	1
A_4	1	1	1	3	1	1	1	1	1	1	1	1
$U(1)_R$	1	1	1	1	1	1	0	0	0	0	0	2
\mathbb{Z}_4	3	3	3	0	0	2	2	0	0	2	1	2
\mathbb{Z}_4	3	3	3	0	2	2	2	0	2	0	1	2
\mathbb{Z}_3	1	2	0	0	1	2	0	0	0	0	2	0
\mathbb{Z}_3	1	1	0	0	2	0	0	0	1	2	2	0
\mathbb{Z}_3	0	2	2	1	0	2	2	0	1	1	2	1
\mathbb{Z}_3	0	0	0	2	0	0	0	0	1	2	1	0

$$\mathcal{W}_\nu = \frac{1}{\Lambda}(H_5 F)(\phi_{23} N_1) + \frac{1}{\Lambda}(H_5 F)(\phi_{102} N_2), \quad (3.2)$$

$$\begin{aligned} \mathcal{W}_d = & \frac{1}{\Lambda^3} \theta_2 \bar{H}_5 F(T_1 \phi_2) H_{24} + \frac{1}{\Lambda^3} \theta_{102} \bar{H}_5 F(T_2 \phi_{102}) H_{24} \\ & + \frac{1}{\Lambda^2} F(T_2 \phi_{23}) \bar{H}_{45} H_{24} + \frac{1}{\Lambda} \bar{H}_5 F(T_3 \phi_3), \end{aligned} \quad (3.3)$$

$$\begin{aligned} \mathcal{W}_u = & \frac{1}{\Lambda^2} T_1^2 H_5 \xi_u \xi_1 + \frac{1}{\Lambda^2} T_1 T_2 H_5 \xi_u^2 + \frac{1}{\Lambda^2} T_2^2 H_5 \xi_1^2 \\ & + \frac{1}{\Lambda} T_2 T_3 H_5 \xi_1 + T_3^2 H_5, \end{aligned} \quad (3.4)$$

where Λ denotes the messenger scale. The flavon potential, which gives rise to the VEVs of the fields ϕ_i , ξ_i , and θ_i will be discussed separately in the next section. Note that the flavons of type ϕ which enter the Yukawa couplings will be aligned with real VEVs while the flavons of type θ and ξ will generally acquire complex VEVs with precisely determined phases. The above superpotential gives rise to the flavor structures in the neutrino sector, in the down-type

TABLE II. The flavon field content of our model.

	$SU(5)$	A_4	$U(1)_R$	\mathbb{Z}_4	\mathbb{Z}_4	\mathbb{Z}_3	\mathbb{Z}_3	\mathbb{Z}_3	\mathbb{Z}_3
ϕ_{102}	1	3	0	0	0	1	0	1	1
ϕ_{23}	1	3	0	2	0	2	1	0	1
ϕ_1	1	3	0	1	3	1	0	0	1
ϕ_2	1	3	0	0	3	0	0	0	0
ϕ_3	1	3	0	1	1	0	0	0	1
ϕ_{111}	1	3	0	3	3	0	0	0	0
ϕ_{211}	1	3	0	0	0	2	1	1	0
ξ_u	1	1	0	0	0	0	2	1	0
ξ_1	1	1	0	0	0	1	2	0	0
ξ_2	1	1	0	0	0	2	0	2	0
θ_2	1	1	0	0	1	0	0	0	0
θ_{102}	1	1	0	0	0	1	0	0	2
ρ_{111}	1	1	0	3	3	0	0	0	0
$\bar{\rho}_{111}$	1	1	0	3	3	0	0	0	0
ρ_{23}	1	1	0	0	0	2	1	0	1
ρ_{102}	1	1	0	0	0	1	0	1	1

quark and charged lepton sectors, and in the up-type quark sector.

Neutrino sector.—From the flavon potential, to be discussed in the next section, the two triplet flavons entering the neutrino Yukawa sector are aligned along the directions

$$\langle \phi_{23} \rangle \sim \begin{pmatrix} 0 \\ 1 \\ -1 \end{pmatrix}, \quad \langle \phi_{102} \rangle \sim \begin{pmatrix} 1 \\ 0 \\ 2 \end{pmatrix}, \quad (3.5)$$

where both alignments are real. Inserting the above vacuum alignments, the real VEV $\langle \xi_1 \rangle$ and the VEV $\langle \xi_2 \rangle$ with a phase of $-\pi/3$ into the superpotential leads to a Dirac-Yukawa matrix and a right-handed heavy Majorana mass matrix of the form

$$Y_\nu = \begin{pmatrix} 0 & b \\ a & 0 \\ -a & 2b \end{pmatrix} \quad \text{and} \quad M_R = \begin{pmatrix} M_A & 0 \\ 0 & M_B \end{pmatrix}, \quad (3.6)$$

where M_A , a and b are real and M_B has a complex phase of $-\pi/3$. The (type I) seesaw formula leads to a simple effective light neutrino mass matrix of the form given in Eq. (2.1) where the relative phase difference α between m_a and m_b is now fixed to be $\pi/3$. This form of M_ν gives $\theta_{13}^\nu \sim 5^\circ - 6^\circ$ for the 1–3 mixing in the neutrino sector, which will finally add up with the charged lepton mixing contribution.

Down-type quark and charged lepton sector.—Turning to the down quark and charged lepton sector, two further triplet flavons enter,

$$\langle \phi_2 \rangle \sim \begin{pmatrix} 0 \\ 1 \\ 0 \end{pmatrix}, \quad \langle \phi_3 \rangle \sim \begin{pmatrix} 0 \\ 0 \\ 1 \end{pmatrix}, \quad (3.7)$$

where $\langle \phi_2 \rangle$ is aligned to be real. The phase of $\langle \phi_3 \rangle$ will turn out to be unphysical. Furthermore the singlet θ_2 with a phase of $\pi/2$ and the singlet θ_{102} with a phase of $4\pi/3$ enters. Plugging in the VEVs of the flavon fields leads to the following structure of the Yukawa matrices (in left-right convention) for the down-type quarks and charged leptons:

$$\begin{aligned} Y_d = & \begin{pmatrix} 0 & i\epsilon_2 & 0 \\ \bar{\omega}\epsilon_{102} & \epsilon_{23} & 2\bar{\omega}\epsilon_{102} - \epsilon_{23} \\ 0 & 0 & \epsilon_3 \end{pmatrix} \quad \text{and} \\ Y_e = & \begin{pmatrix} 0 & -3/2\bar{\omega}\epsilon_{102} & 0 \\ -3/2i\epsilon_2 & 9/2\epsilon_{23} & 0 \\ 0 & (-3\bar{\omega}\epsilon_{102} - 9/2\epsilon_{23}) & \epsilon_3 \end{pmatrix}, \end{aligned} \quad (3.8)$$

where $\bar{\omega} = e^{4\pi i/3}$; cf. Sec. II. The ϵ_i are proportional to the order one couplings which we have not written down explicitly and possible Higgs mixing angles. For the sake of simplicity we only show here the proportionality to the dimensionful quantities

$$\begin{aligned}\epsilon_2 &\sim \frac{v_{24}}{\Lambda^3} |\langle \theta_2 \rangle \langle \phi_2 \rangle|, & \epsilon_{102} &\sim \frac{v_{24}}{\Lambda^3} |\langle \theta_{102} \rangle \langle \phi_{102} \rangle|, \\ \epsilon_{23} &\sim \frac{v_{24}}{\Lambda^2} |\langle \phi_{23} \rangle|, & \epsilon_3 &\sim \frac{1}{\Lambda} |\langle \phi_3 \rangle|,\end{aligned}\quad (3.9)$$

where v_{24} is the VEV of H_{24} . We also note that we do not use the common Georgi-Jarlskog relation $m_\mu/m_s = 3$ [28] at the GUT scale but rather $m_\mu/m_s = 9/2$ [34,35]. The reason for this is that recent lattice results (see, e.g., [36]) suggest a much smaller error for the strange quark mass than the Particle Data Group (PDG) quotes. And since we are in the small $\tan \beta$ regime and no large supersymmetry (SUSY) threshold corrections can correct the second generation GUT scale Yukawa coupling ratios we have to use the more realistic relation mentioned above. Explicitly, from the VEVs of H_{24} and \bar{H}_5 we get a relative factor of $-3/2$ for ϵ_2 and ϵ_{102} and the $9/2$ from H_{24} and \bar{H}_{45} . For the third generation we use $b - \tau$ Yukawa unification which is possible for small $\tan \beta$ due to the large renormalisation group equation (RGE) effects induced by the top mass.

For the 1–2 mixing in the charged lepton sector, we nevertheless obtain $\theta_{12}^e \approx \theta_c/3$, where $\theta_c \approx 0.23$ is the Cabibbo angle. The corresponding phase δ_{12}^e is chosen (see Sec. II and Appendix A for conventions), such that the charged lepton mixing angle correction θ_{12}^e is in phase with the neutrino reactor angle θ_{13}^ν and the two angles add together constructively to yield the physical reactor angle θ_{13} .

Up-type quark sector.—Finally the up-type quark sector only involves singlet flavons with real VEVs and gives a real symmetric Yukawa matrix of the form

$$Y_u = \begin{pmatrix} a_u & b_u & 0 \\ b_u & c_u & d_u \\ 0 & d_u & e_u \end{pmatrix}, \quad (3.10)$$

where the dependence on Λ and the flavon VEVs reads

$$\begin{aligned}a_u &\sim \frac{|\langle \xi_u \rangle \langle \xi_1 \rangle|}{\Lambda^2}, & b_u &\sim \frac{|\langle \xi_u \rangle|^2}{\Lambda^2}, \\ c_u &\sim \frac{|\langle \xi_1 \rangle|^2}{\Lambda^2}, & d_u &\sim \frac{|\langle \xi_u \rangle|}{\Lambda}.\end{aligned}\quad (3.11)$$

Note that e_u is coming from a renormalizable coupling and we have not explicitly written down all coefficients. For instance, Λ is only a simplified notation for the various messenger masses as given in Appendix B, and hence $a_u^2 \ll |b_u c_u|$ as in our numerical fit in Sec. VI is possible. The zero texture in the quark sector means that we can successfully apply the quark phase sum rule of [33] due to our choice of phases.

IV. THE VACUUM ALIGNMENT

We have in total seven flavon fields which transform as triplets under A_4 (see Table II) pointing in the following directions in flavor space:

$$\langle \phi_1 \rangle \sim \begin{pmatrix} 1 \\ 0 \\ 0 \end{pmatrix}, \quad \langle \phi_2 \rangle \sim \begin{pmatrix} 0 \\ 1 \\ 0 \end{pmatrix}, \quad \langle \phi_3 \rangle \sim \begin{pmatrix} 0 \\ 0 \\ 1 \end{pmatrix}, \quad (4.1)$$

$$\langle \phi_{211} \rangle \sim \begin{pmatrix} -2 \\ 1 \\ 1 \end{pmatrix}, \quad \langle \phi_{111} \rangle \sim \begin{pmatrix} 1 \\ 1 \\ 1 \end{pmatrix}, \quad \langle \phi_{23} \rangle \sim \begin{pmatrix} 0 \\ 1 \\ -1 \end{pmatrix}. \quad (4.2)$$

Apart from $\langle \phi_1 \rangle$ and $\langle \phi_3 \rangle$, the VEVs of the above listed flavons will be aligned real using the phase alignment mechanism proposed in [22]. The phases of $\langle \phi_1 \rangle$ and $\langle \phi_3 \rangle$ have no physical implications and hence will be set real for definiteness. The first three VEVs form a basis in flavor space, while the second three alignments are proportional to the (real) columns of the tri-bimaximal mixing matrix. In our model, instead of ϕ_{111} (which is used in the CSD [18,19] models), we require the following (real) alignment:

$$\langle \phi_{102} \rangle \sim \begin{pmatrix} 1 \\ 0 \\ 2 \end{pmatrix}, \quad (4.3)$$

in the neutrino sector, similar to a recently proposed flavon alignment [17] but with the phase fixed as explicitly shown and discussed below.

The principal assumption of our model is that CP is conserved above the flavor breaking scale, and is spontaneously broken by the CP violating phases of flavon fields. With this assumption we can not only reproduce the correct mixing angles but can also make definite testable predictions for the CP violating phases in the lepton sector. In order to do this we will fix the phases of the following flavon VEVs to

$$\alpha_{111} = 0, \quad \alpha_{211} = 0, \quad \alpha_{23} = 0, \quad \alpha_2 = 0, \quad \alpha_{102} = 0, \quad (4.4)$$

where α_i stands for the phase of $\langle \phi_i \rangle$. Furthermore we have some singlet flavons with nonvanishing VEVs of which some will have nontrivial phases. In this choice we have also ignored possible signs which means that the phases are fixed up to $\pm \pi$. We can fix the phases by using appropriate \mathbb{Z}_n shaping symmetries as described in our previous paper [22]; see also Sec. II.

The method can be understood easily for the A_4 singlet flavon VEVs. Their superpotential reads

$$\begin{aligned}\mathcal{W} &= \frac{P}{\Lambda} (\xi_1^3 - M^3) + \frac{P}{\Lambda} (\xi_2^3 + M^3) + \frac{P}{\Lambda} (\xi_u^3 - M^3) \\ &+ \frac{P}{\Lambda^2} (\theta_2^4 - M^4) + \frac{P}{\Lambda} (\theta_{102}^3 - M^3) \\ &+ \frac{P}{\Lambda} (\rho_{102}^3 - M^3) + \frac{P}{\Lambda} (\rho_{23}^3 - M^3),\end{aligned}\quad (4.5)$$

where M is a generic mass scale which we assume to be positive. The list of the driving fields is given in Table III. The F terms for P will then fix the flavon VEVs of the singlets up to a discrete choice. Note that for the sake of simplicity we have only introduced one P field. Indeed, we need one P field for every singlet. Since they all have the same quantum numbers they will mix and we can go to a basis where all terms are disentangled as in the equation above; see the Appendix of [22]. For the singlet flavons here we choose $\langle \xi_{1,u} \rangle$ and $\langle \rho_{102,23} \rangle$ to be real, $\langle \theta_2 \rangle$ to be imaginary, $\langle \theta_{102} \rangle$ to have a phase of $4\pi/3$ and $\langle \xi_2 \rangle$ to have a phase of $-\pi/3$.

We come now back to the phases of the triplet flavon VEVs which can be fixed in the same way after the direction in flavor space is fixed. Note that the phases α_1 and α_3 are not fixed in our model. This is also not necessary. The flavon ϕ_1 does not couple to the matter sector and hence its phase does not appear in the mass matrices. It will only be used in orthogonality relations where the phase of the VEV does not matter. The flavon ϕ_3 couples nevertheless to the matter sector. But as we have seen before it determines the 3–3 element of the down-type quark and charged lepton Yukawa matrix and its phase can be absorbed in the right-handed fields such that this phase renders unphysical.

In this section we will use an explicit notation for the contraction of the A_4 indices. We use the standard “ $SO(3)$ basis” for which the singlet of $\mathbf{3} \otimes \mathbf{3}$ is given by the $SO(3)$ -type inner product “ \cdot .” The two triplets of $\mathbf{3} \otimes \mathbf{3}$ are constructed from the usual (antisymmetric) cross product “ \times ” and the symmetric star product “ \star ” (see, for example, [26]).

TABLE III. The driving field content of our model. Note that we only show here one P field. Indeed one has to introduce as many P fields as operators to fix the phases of the flavon fields. Since they will have all the same quantum numbers they will mix and we can go to a basis where the terms to fix the phase for each flavon is separated from the others. This was discussed in the Appendix of [22].

	$SU(5)$	A_4	$U(1)_R$	\mathbb{Z}_4	\mathbb{Z}_4	\mathbb{Z}_3	\mathbb{Z}_3	\mathbb{Z}_3	\mathbb{Z}_3
$O_{1;2}$	1	1	2	3	2	2	0	0	2
$O_{1;3}$	1	1	2	2	0	2	0	0	1
$O_{2;3}$	1	1	2	3	0	0	0	0	2
$O_{111;211}$	1	1	2	1	1	1	2	2	0
$O_{111;23}$	1	1	2	3	1	1	2	0	2
$O_{23;211}$	1	1	2	2	0	2	1	2	2
$O_{2;102}$	1	1	2	0	1	2	0	2	2
$O_{211;102}$	1	1	2	0	0	0	2	1	2
$O_{1;23}$	1	1	2	1	1	0	2	0	1
A_1	1	3	2	2	2	1	0	0	1
A_2	1	3	2	0	2	0	0	0	0
A_3	1	3	2	2	2	0	0	0	1
A_{111}	1	3	2	2	2	0	0	0	0
P	1	1	2	0	0	0	0	0	0

We start with the alignment of the triplet flavons ϕ_i , $i = 1, 2, 3$, which can be aligned via

$$\mathcal{W} = A_i \cdot (\phi_i \star \phi_i) + O_{i;j}(\phi_i \cdot \phi_j) + \frac{P}{\Lambda^2}((\phi_2 \cdot \phi_2)^2 - M^4). \quad (4.6)$$

Solving the F -term conditions of A_i aligns the flavons in one of the three standard directions and the F -term conditions of $O_{i;j}$ makes them orthogonal to each other. By convention we let them point in the directions as given in Eq. (4.1). For α_2 we choose the value 0 (α_1 and α_3 remain undetermined). In Appendix B we will discuss the messenger sector of our model. After integrating out heavy messenger fields we end up only with the effective operators written here and in the following.

We now turn to the flavons ϕ_{23} , ϕ_{111} , and ϕ_{211} : For ϕ_{111} we use a slight modification of the alignment in the recent $SU(5) \times T'$ model [13] without auxiliary flavons,

$$\mathcal{W} = A_{111} \cdot (\phi_{111} \star \phi_{111} + \phi_{111} \rho_{111} + \phi_{111} \tilde{\rho}_{111}) + \frac{P}{\Lambda^2}((\phi_{111} \cdot \phi_{111})^2 - M^4) + \frac{P}{\Lambda^2}(\rho_{111}^4 + \rho_{111}^2 \tilde{\rho}_{111}^2 + \tilde{\rho}_{111}^4 - M^4). \quad (4.7)$$

It gives the desired alignment and $\langle \phi_{111} \rangle$ can be chosen to be real.

Starting from this the other two alignments can be realized by

$$\mathcal{W} = O_{1;23}(\phi_1 \cdot \phi_{23}) + O_{111;23}(\phi_{111} \cdot \phi_{23}) + O_{111;211}(\phi_{111} \cdot \phi_{211}) + O_{23;211}(\phi_{23} \cdot \phi_{211}) + \frac{P}{\Lambda}((\phi_{211} \star \phi_{211}) \cdot \phi_{211} - M^3) + \frac{P}{\Lambda}((\phi_{23} \cdot \phi_{23})\rho_{23} - M^3). \quad (4.8)$$

The orthogonality gives the desired directions and $\langle \phi_{211} \rangle$ can be chosen to be real. The phase of $\langle \phi_{23} \rangle$ is a bit peculiar. Above we have fixed $\langle \rho_{23} \rangle$ to be real and hence also $\langle \phi_{23} \rangle$ can be chosen to be real. In the first operator the VEV of ϕ_1 enters again and independent of the phases a $(0, 1, -1)$ alignment is always orthogonal to a $(1, 0, 0)$ alignment.

Now we have everything together for the last missing nontrivial alignment

$$\mathcal{W} = O_{211;102}(\phi_{102} \cdot \phi_{211}) + O_{2;102}(\phi_{102} \cdot \phi_2) + \frac{P}{\Lambda}((\phi_{102} \cdot \phi_{102})\rho_{102} - M^3). \quad (4.9)$$

The direction is again fixed by orthogonality conditions. The VEV of ϕ_{102} can be chosen to be real (remember that also $\langle \rho_{102} \rangle$ is real).

V. THE HIGGS MASS

In our model we assume $b - \tau$ Yukawa coupling unification at the GUT scale. This happens in the minimal supersymmetric standard model (MSSM) only for large $\tan \beta$ via SUSY threshold corrections or small $\tan \beta$ due to large RGE corrections by the top mass. We have decided for the second solution such that we can also neglect SUSY threshold corrections in our fit later on.

Nevertheless, the MSSM with small $\tan \beta$ prefers very light Higgs masses which is in conflict with the recent discovery of a Higgs-like particle with a mass of about 126 GeV [37].

A possible solution to this problem is given by the next-to-minimal supersymmetric standard model (NMSSM); for a review see [38] where the Higgs can have the right mass even for small $\tan \beta$. In fact our symmetries forbid a μ -term because the combinations $H_5 \bar{H}_5$ and $H_{45} \bar{H}_{45}$ are charged under the shaping symmetries. But we have checked that we can add a singlet field S which couples simultaneously to this two combinations. For convenience we have listed the field S in Table I.

An explicit S^3 -term in the superpotential is forbidden in the limit of unbroken $U(1)_R$ symmetry (i.e., before SUSY breaking) and by the shaping symmetries but is needed to stabilize the Higgs potential in the scale invariant NMSSM. But we note that there are still various possibilities to stabilize the potential for S . This could be done, for instance, by introducing an additional $U(1)'$ gauge group where the potential is stabilized by the $U(1)'$ D -terms. For a description of this and references, see the review article [38]. We only note that it is straightforward to introduce such a $U(1)'$ in our model by charging the Higgs and matter fields appropriately which does not alter the flavor sector. Alternatively, the S^3 term could be generated nonperturbatively, breaking the shaping symmetries in an F -theory framework; see, for instance, [39]. We will not go here into more detail on this model building aspect and only like to note that our flavor model is compatible with some NMSSM variants and hence we can have a realistic Higgs mass.

VI. THE FIT AND NUMERICAL RESULTS

Here we will present the results of a numerical χ^2 -fit of the high energy parameters of the Yukawa matrices to the low energy charged lepton and quark masses and quark mixing parameters. Afterwards we will present the predictions for neutrino masses and mixing.

For the RGE running of the Yukawa matrices we have used the REAP package [40] and calculated with it the masses and mixing angles at low energies. Note that we have used the RGEs of the MSSM. Possible RGE effects due to including a variant of the NMSSM are neglected. On the one hand we can expect this effect to be flavor blind

$$\chi^2/\text{dof} = 2.05/3$$

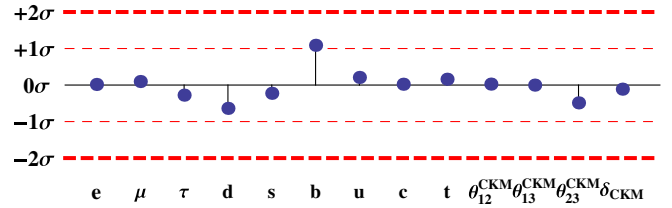


FIG. 1 (color online). Pictorial representation of the deviation of our predictions from low energy experimental data for the charged lepton Yukawa couplings and quark Yukawa couplings and mixing parameters. The deviations of the charged lepton masses are given in 1% while all other deviations are given in units of standard deviations σ .

leading only to a rescaling of the GUT scale parameters and on the other hand, in the scale-invariant NMSSM for example, the RGE effects come from the coupling λ which can be small [41] although $\tan \beta$ given there is preferred to be larger than 10. For small $\tan \beta$ the coupling λ has to be rather large to be in agreement with recent Higgs data; see, e.g., [42]. Furthermore, SUSY threshold corrections are negligibly small due to the small $\tan \beta$ and hence are not included in the fit.

For the charged lepton and quark masses and their errors at the top scale $m_t(m_t)$ we have taken the values from [43] and for the Cabibbo-Kobayashi-Maskawa (CKM) parameters the PDG values [44]. Note that the experimental errors for the charged lepton masses are tiny and we have estimated the theoretical uncertainty from higher order effects to 1%, and we will assume this as their errors instead.

The Yukawa matrices depend on nine real parameters (five from the up-type quarks and four from the down-type quarks and charged leptons). Furthermore we have included $\tan \beta$ as a free parameter in the fit. The unification of the b and the τ Yukawa coupling at the GUT scale depends strongly on this parameter. On the contrary, the masses and mixing angles depend only very weakly on the SUSY scale which we have therefore fixed to $M_{\text{SUSY}} = 750$ GeV.

The fit results are summarized in Fig. 1 and Tables IV and V. We have fitted ten parameters to thirteen observables with a χ^2 of 2.05 and hence we can say that our model describes the data very well.⁶ Note that we followed here

⁶We note that while we get an excellent fit for the quark masses themselves, as given in the PDG review, there is some tension with QCD results which favour $y_s/y_d \approx 19$ [45], while our fit yields $y_s/y_d = 25.3$. We remark that this tension is the same that one also gets with the more conventional Georgi-Jarlskog relation instead of the Clebsch factors 9/2 and 3/2 used here, so it is not particular for our model. In our fit, we have not included y_s/y_d as constraints, but we would like to note that future even more precise results on the quark masses, including lattice results, can provide powerful additional constraints on unified flavor models.

TABLE IV. Values of the effective parameters of the quark and charged lepton Yukawa matrices and $\tan\beta$ for $M_{\text{SUSY}} = 750$ GeV. The numerical values are determined from a χ^2 -fit to experimental data with a χ^2 per degree of freedom of 2.05/3.

Parameter	Value
a_u	-3.01×10^{-5}
b_u	-2.66×10^{-4}
c_u	-2.57×10^{-3}
d_u	3.09×10^{-2}
e_u	2.05
ϵ_2	-3.57×10^{-5}
ϵ_{102}	3.17×10^{-5}
ϵ_{23}	1.62×10^{-4}
ϵ_3	1.24×10^{-2}
$\tan\beta$	1.49

the strategy of our previous paper [33] where we have found that for Yukawa matrices with negligibly small 1–3 mixings we find the correct value for the CKM phase and the Cabibbo angle θ_C with $\theta_{12}^d \approx \epsilon_2/\epsilon_{23} \lesssim \theta_C$ and $\theta_{12}^u \approx b_u/c_u \approx \theta_C/2$ if these two angles have a relative phase difference of 90° .

We turn our discussion now to the neutrino sector. Here we did not fit the parameters to the observables because here we are more interested in the allowed ranges and correlations between different observables which help in distinguishing this model from other models.

The effective neutrino mass matrix from Eq. (2.1) depends on three parameters. The neutrino mass scale m_a the perturbation parameter ϵ and the relative phase α . The phase α in our model is $\pi/3$ as discussed in Sec. II. Hence, only two real parameters m_a and ϵ completely determine all observables in the neutrino sector.

We have varied these two parameters randomly and the results are shown in Fig. 2 where we have used as constraint the fit results of the Bari group [31]. The blue dots agree with all experimental data within 3σ while the red dots agree even within 1σ . The dashed lines in the plots label the corresponding allowed ranges of the observables on the axes. The 1σ range of the leptonic Dirac phase δ is shown in black because it is not measured directly and the fit results should be taken with a grain of salt. In the scan we also did not include it as a constraint.

We are everywhere in good agreement with the experimental data and we find clear correlations. Especially, noteworthy is the value for θ_{23} which lies around 38.5° . We also make precise predictions for the CP violating phases. One of the Majorana phases is unphysical because one neutrino remains massless. The Dirac CP phase has a value of $\delta \approx 130^\circ$ and the physical Majorana phase is $\alpha_2 \approx 315^\circ$. The Jarlskog determinant J_{CP} is around 0.025 and the effective neutrino mass for neutrinoless double beta decay m_{ee} is of the order of 3×10^{-3} eV, beyond the reach of current experiments.

 TABLE V. Fit results for the quark Yukawa couplings and mixing and the charged lepton Yukawa couplings at low energy compared to experimental data. The values for the Yukawa couplings are extracted from [43] and the CKM parameters from [44]. Note that the experimental uncertainty on the charged lepton Yukawa couplings are negligible small and we have assumed a relative uncertainty of 1% for them. The χ^2 per degree of freedom is 2.05/3. A pictorial representation of the agreement between our predictions and experiment can be found as well in Fig. 1.

Quantity [at $m_i(m_i)$]	Experiment	Model	Deviation
y_τ in 10^{-2}	1.00	1.00	-0.277
y_μ in 10^{-4}	5.89	5.89	0.097
y_e in 10^{-6}	2.79	2.79	-0.016
y_b in 10^{-2}	1.58 ± 0.05	1.64	1.088
y_s in 10^{-4}	2.99 ± 0.86	2.95	-0.226
y_d in 10^{-6}	$15.9^{+6.8}_{-6.6}$	11.7	-0.639
y_t	0.936 ± 0.016	0.939	0.159
y_c in 10^{-3}	3.39 ± 0.46	3.40	0.223
y_u in 10^{-6}	$7.01^{+2.76}_{-2.30}$	7.59	0.209
θ_{12}^{CKM}	$0.2257^{+0.0009}_{-0.0010}$	0.2257	0.026
θ_{23}^{CKM}	$0.0415^{+0.0011}_{-0.0012}$	0.0409	-0.488
θ_{13}^{CKM}	0.0036 ± 0.0002	0.0036	-0.002
δ_{CKM}	$1.2023^{+0.0786}_{-0.0431}$	1.1975	-0.113

VII. SUMMARY

We have constructed a unified $A_4 \times SU(5)$ model featuring the new type of constrained sequential dominance CSD2 proposed recently in [17]. The $A_4 \times SU(5)$ model, with the CSD2 vacuum alignments $(0, 1, 1)^T$ and $(1, 0, 2)^T$, provides an excellent fit to the present data on quark and lepton masses and mixings, including the measured value of the leptonic mixing angle θ_{13} from Daya Bay and RENO, with testable predictions for the yet unknown parameters of the leptonic mixing matrix.

The main idea of the present model is that, with a strong normal hierarchical spectrum (with $m_1^\nu = 0$ by construction since there are only two right-handed neutrinos) the 1–3 angle in the neutrino sector, θ_{13}^ν , is related to a ratio of neutrino masses by $\theta_{13}^\nu = \frac{\sqrt{2}}{3} \frac{m_2^\nu}{m_3^\nu}$, leading to $\theta_{13}^\nu \sim 5^\circ - 6^\circ$. In addition, the reactor angle receives another contribution from mixing in the charged lepton sector. The charged lepton mixing induces a correction to θ_{13} of $\sim 3^\circ$ which adds up constructively with θ_{13}^ν to give

$$\theta_{13} \sim 8^\circ - 9^\circ, \quad (7.1)$$

within the range of the measured value from Daya Bay and RENO. The constructive addition of the neutrino and charged lepton mixing angles is achieved by assuming high energy CP invariance which is spontaneously broken by flavon fields whose phases are controlled using Abelian \mathbb{Z}_3 and \mathbb{Z}_4 symmetries as proposed in [22]. We emphasize that in our approach

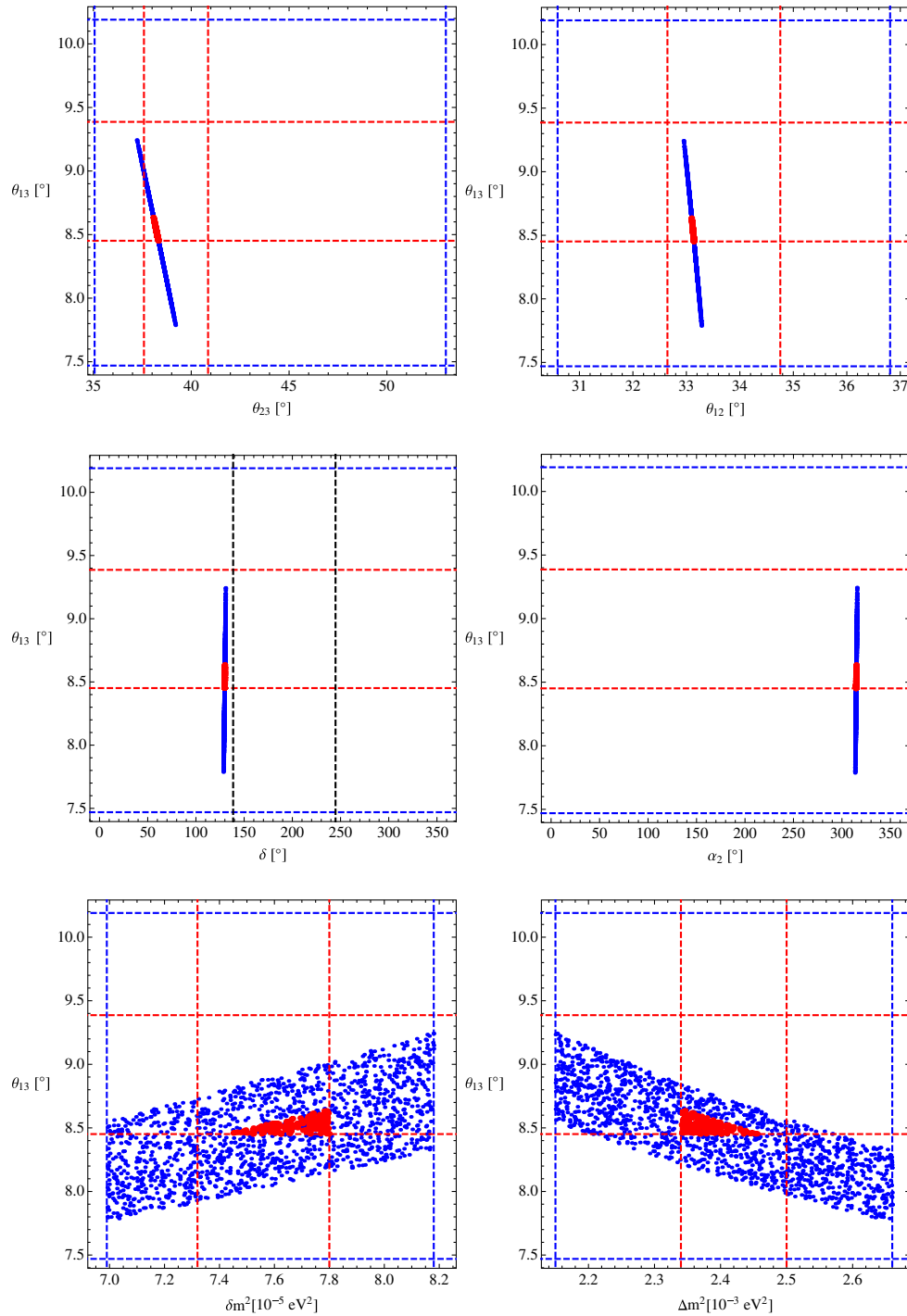


FIG. 2 (color online). The correlations between θ_{13} and the other two mixing angles and the two physical phases in PCSD2. The regions compatible with the 1σ (3σ) ranges of the mass squared differences and the mixing angles, taken from [31], are depicted by the red (blue) points and delimited by dashed lines in corresponding colours. The 1σ region for the Dirac CP phase is shown in black.

one can either use a “simple” CP symmetry, under which the components of the scalar fields transform trivially as $\phi_i \rightarrow \phi_i^*$, or a generalized CP symmetry (see, e.g., [27] and references therein) where, in our basis, the triplet fields would transform as $\phi_i \rightarrow U_3 \phi_i^*$, with U_3 interchanging the second and third component of a triplet representation.

The resulting unified flavor model is highly predictive, as described in Sec. VI, since only two parameters determine the neutrino mass matrix, while the charged lepton corrections are fixed by the GUT framework: In particular, for the Dirac CP phase δ , for the one physical Majorana CP phase α_2 and for the atmospheric angle θ_{23} we obtain the predictions

$$\delta \approx 130^\circ, \quad \alpha_2 \approx 315^\circ, \quad \text{and} \quad \theta_{23} \approx 38.5^\circ. \quad (7.2)$$

The predictions for δ and θ_{23} will be tested by the ongoing and future neutrino oscillation experiments. In addition, for θ_{12} , we predict a value of

$$\theta_{12} \sim 33^\circ, \quad (7.3)$$

which is slightly smaller than the tri-bimaximal mixing value but may be tested by a future reactor experiment with ~ 60 km baseline, which could measure θ_{12} with much improved precision [32]. Furthermore, in the quark sector, we obtain a right-angled unitarity triangle (with $\alpha \approx 90^\circ$) from the same vacuum alignment techniques for the phases [22], realizing the phase sum rule of [33].

In summary, we have presented a highly predictive new unified model for fermion masses and mixing, which, in fact, represents the first unified indirect family symmetry model in the literature that has been constructed to date that is consistent with all experimental data on quark and lepton mass and mixing angles, and makes definite predictions for CP phases in both the quark and lepton sectors.

ACKNOWLEDGMENTS

We thank Michael A. Schmidt and Martin Holthausen for useful discussions about A_4 and generalized CP transformations and Christoph Luhn for useful discussions during the early stages of the project. S.A. acknowledges support by the Swiss National Science Foundation, S.F.K. from the STFC Consolidated Grant No. ST/J000396/1, and M.S. by the ERC Advanced Grant No. 267985:“DaMESyFla.” S.F.K. and M.S. also acknowledge partial support from the EU Marie Curie ITN UNILHC (Grant No. PITN-GA-2009-237920) and all authors were partially supported by the European Union under FP7 ITN INVISIBLES (Marie Curie Actions, Grant No. PITN-GA-2011-289442).

APPENDIX A: CONVENTIONS AND NOTATIONS

In this section we want to summarize briefly our conventions and define some notation used throughout the main text. We will follow mainly the notation of [30]. The only difference is a sign in the Majorana phases.

The Yukawa couplings follow the left-right convention

$$\mathcal{L}_{\text{Yuk}} = -Y_{ij} \bar{\psi}_L^i \psi_R^j H + \text{H.c.}, \quad (A1)$$

and for the effective light neutrino mass matrix we use the convention

$$\mathcal{L}_\nu = -\frac{1}{2} \bar{L}_i (M_\nu)_{ij} L_j^c + \text{H.c.}, \quad (A2)$$

where L is the lepton doublet.

In the quark sector we define the CKM matrix by

$$U_{\text{CKM}} = U_u U_d^\dagger = R_{23} U_{13} R_{12}, \quad (A3)$$

where U_u (U_d) is a unitary matrix diagonalizing $Y_u Y_u^\dagger$ ($Y_d Y_d^\dagger$) and

$$U_{12} = \begin{pmatrix} c_{12} & s_{12} e^{-i\delta_{12}} & 0 \\ -s_{12} e^{i\delta_{12}} & c_{12} & 0 \\ 0 & 0 & 1 \end{pmatrix}, \quad (A4)$$

and similar for U_{23} and U_{13} . We use c_{12} and s_{12} as abbreviations for $\cos \theta_{12}$ and $\sin \theta_{12}$. The matrices R_{23} and R_{12} are U_{23} and U_{12} with the complex phases set to zero. In this case δ_{13} coincides with the CKM phase δ_{CKM} .

For the Pontecorvo-Maki-Nakagawa-Sakata (PMNS) matrix we use

$$U_{\text{PMNS}} = U_e U_\nu^\dagger = R_{23} U_{13} R_{12} \text{diag}(e^{-i\alpha_1/2}, e^{-i\alpha_2/2}, 1), \quad (A5)$$

where the neutrino mass matrix is diagonalized via

$$U_\nu M_\nu M_\nu^\dagger U_\nu^\dagger = \text{diag}(m_1^2, m_2^2, m_3^2) \quad (A6)$$

and $U_\nu^\dagger = U_{23}^\nu U_{13}^\nu U_{12}^\nu$ (note the Hermitian conjugation). This conventions imply a complex conjugation of the neutrino mass matrix M_ν compared to our previous CSD2 paper [17] and also the sign of the Majorana phases here is different.

APPENDIX B: THE RENORMALIZABLE SUPERPOTENTIAL

In this appendix we discuss the full renormalizable superpotential including the messenger fields which after being integrated out give the effective operators as discussed before.

We start with the superpotential bilinear in the fields which is in our case only the mass terms for the messengers

$$\begin{aligned} \mathcal{W}_\Lambda^{\text{ren}} = & M_{\Sigma_i} \Sigma_i \bar{\Sigma}_i + M_{Y_i} Y_i \bar{Y}_i + M_{\Xi_i} \Xi_i \bar{\Xi}_i \\ & + M_{\Omega_i} \Omega_i \bar{\Omega}_i + M_{\Gamma_i} \Gamma_i \bar{\Gamma}_i. \end{aligned} \quad (B1)$$

The full list of messenger fields is given in Table VI where every line is a messenger pair which receives a mass larger than the GUT scale so that they can be integrated out to give the desired effective operators. To simplify the notation before we have introduced the messenger scale Λ as shorthand which is related to the individual messenger masses with order one coefficients.

Note that in the superpotential bilinear in the fields no μ -term for the Higgs fields appears. This term is forbidden by symmetries and in combination with a NMSSM like mechanism helps to increase the Higgs mass to the experimentally determined value. A possible singlet field S with couplings $S(H_5 \bar{H}_5 + H_{45} \bar{H}_{45})$ would not appear anywhere else in the superpotential with the symmetries and field content as specified in Tables I, II, III, and VI.

TABLE VI. The messenger field content of our model. Every line represents a messenger pair which receives a mass larger than the GUT scale and no cross terms are allowed. In the main text we labeled the messenger mass scale generically with Λ .

	$SU(5)$	A_4	$U(1)_R$	\mathbb{Z}_4	\mathbb{Z}_4	\mathbb{Z}_3	\mathbb{Z}_3	\mathbb{Z}_3	\mathbb{Z}_3
$\Sigma_1, \bar{\Sigma}_1$	$\mathbf{5}, \bar{\mathbf{5}}$	$\mathbf{1}, \mathbf{1}$	1, 1	2, 2	0, 0	1, 2	2, 1	2, 1	0, 0
$\Sigma_2, \bar{\Sigma}_2$	$\mathbf{5}, \bar{\mathbf{5}}$	$\mathbf{1}, \mathbf{1}$	1, 1	0, 0	0, 0	2, 1	0, 0	1, 2	0, 0
$\Sigma_3, \bar{\Sigma}_3$	$\mathbf{5}, \bar{\mathbf{5}}$	$\mathbf{1}, \mathbf{1}$	1, 1	3, 1	3, 1	0, 0	0, 0	2, 1	0, 0
Y_1, \bar{Y}_1	$\mathbf{10}, \bar{\mathbf{10}}$	$\mathbf{3}, \mathbf{3}$	1, 1	1, 3	3, 1	1, 2	2, 1	2, 1	1, 2
Y_2, \bar{Y}_2	$\mathbf{10}, \bar{\mathbf{10}}$	$\mathbf{3}, \mathbf{3}$	1, 1	3, 1	3, 1	0, 0	1, 2	0, 0	1, 2
Y_3, \bar{Y}_3	$\mathbf{10}, \bar{\mathbf{10}}$	$\mathbf{3}, \mathbf{3}$	1, 1	3, 1	2, 2	1, 2	1, 2	0, 0	0, 0
$\Xi_1, \bar{\Xi}_1$	$\mathbf{5}, \bar{\mathbf{5}}$	$\mathbf{3}, \mathbf{3}$	1, 1	3, 1	3, 1	1, 2	1, 2	0, 0	0, 0
$\Xi_2, \bar{\Xi}_2$	$\mathbf{5}, \bar{\mathbf{5}}$	$\mathbf{3}, \mathbf{3}$	1, 1	3, 1	3, 1	0, 0	1, 2	0, 0	1, 2
$\Xi_3, \bar{\Xi}_3$	$\mathbf{5}, \bar{\mathbf{5}}$	$\mathbf{3}, \mathbf{3}$	1, 1	3, 1	2, 2	1, 2	1, 2	0, 0	0, 0
$\Omega_1, \bar{\Omega}_1$	$\mathbf{10}, \bar{\mathbf{10}}$	$\mathbf{1}, \mathbf{1}$	1, 1	3, 1	3, 1	1, 2	2, 1	2, 1	0, 0
$\Omega_2, \bar{\Omega}_2$	$\mathbf{10}, \bar{\mathbf{10}}$	$\mathbf{1}, \mathbf{1}$	1, 1	3, 1	3, 1	1, 2	0, 0	1, 2	0, 0
$\Omega_3, \bar{\Omega}_3$	$\mathbf{10}, \bar{\mathbf{10}}$	$\mathbf{1}, \mathbf{1}$	1, 1	3, 1	3, 1	2, 1	2, 1	1, 2	0, 0
$\Gamma_1, \bar{\Gamma}_1$	$\mathbf{1}, \mathbf{1}$	$\mathbf{1}, \mathbf{1}$	0, 2	0, 0	0, 0	2, 1	0, 0	0, 0	1, 2
$\Gamma_2, \bar{\Gamma}_2$	$\mathbf{1}, \mathbf{1}$	$\mathbf{1}, \mathbf{1}$	0, 2	0, 0	0, 0	2, 1	0, 0	2, 1	2, 1
$\Gamma_3, \bar{\Gamma}_3$	$\mathbf{1}, \mathbf{1}$	$\mathbf{1}, \mathbf{1}$	0, 2	0, 0	0, 0	1, 2	2, 1	0, 0	2, 1
$\Gamma_4, \bar{\Gamma}_4$	$\mathbf{1}, \mathbf{1}$	$\mathbf{1}, \mathbf{1}$	0, 2	0, 0	0, 0	2, 1	1, 2	0, 0	0, 0
$\Gamma_5, \bar{\Gamma}_5$	$\mathbf{1}, \mathbf{1}$	$\mathbf{1}, \mathbf{1}$	0, 2	0, 0	0, 0	1, 2	0, 0	1, 2	0, 0
$\Gamma_6, \bar{\Gamma}_6$	$\mathbf{1}, \mathbf{1}$	$\mathbf{3}, \mathbf{3}$	0, 2	0, 0	0, 0	1, 2	2, 1	2, 1	0, 0
$\Gamma_7, \bar{\Gamma}_7$	$\mathbf{1}, \mathbf{1}$	$\mathbf{1}, \mathbf{1}$	0, 2	2, 2	2, 2	0, 0	0, 0	0, 0	0, 0
$\Gamma_8, \bar{\Gamma}_8$	$\mathbf{1}, \mathbf{1}$	$\mathbf{1}, \mathbf{1}$	0, 2	0, 0	2, 2	0, 0	0, 0	0, 0	0, 0
$\Gamma_9, \bar{\Gamma}_9$	$\mathbf{1}, \mathbf{1}$	$\mathbf{1}, \mathbf{1}$	0, 2	0, 0	0, 0	0, 0	1, 2	2, 1	0, 0

The next step in our discussion of the renormalizable superpotential is the flavon sector. The full potential for this sector reads (dropping for the sake of simplicity order one coefficients)

$$\begin{aligned}
 \mathcal{W}_{\text{flavon}}^{\text{ren}} = & O_{1;2} \phi_1 \phi_2 + O_{1;3} \phi_1 \phi_3 + O_{2;3} \phi_2 \phi_3 + O_{111;211} \phi_{111} \phi_{211} + O_{111;23} \phi_{111} \phi_{23} + O_{23;211} \phi_{23} \phi_{211} + O_{2;102} \phi_2 \phi_{102} \\
 & + O_{211;102} \phi_{211} \phi_{102} + O_{1;23} \phi_1 \phi_{23} + A_1 \phi_1 \phi_1 + A_2 \phi_2 \phi_2 + A_3 \phi_3 \phi_3 + A_{111} (\phi_{111}^2 + \phi_{111} \rho_{111} + \tilde{\phi}_{111} \rho_{111}) \\
 & + P \Gamma_9 \xi_u + \bar{\Gamma}_9 \xi_u^2 + P \Gamma_8^2 + \bar{\Gamma}_8 \phi_2^2 + \bar{\Gamma}_8 \theta_2^2 + P \Gamma_7^2 + \bar{\Gamma}_7 (\phi_{111}^2 + \rho_{111}^2 + \tilde{\rho}_{111}^2) + P \phi_{211} \Gamma_6 + \phi_{211}^2 \bar{\Gamma}_6 + P \xi_2 \Gamma_5 \\
 & + \xi_2^2 \bar{\Gamma}_5 + P \xi_1 \Gamma_4 + \xi_1^2 \bar{\Gamma}_4 + P \rho_{23} \Gamma_3 + (\phi_{23}^2 + \rho_{23}^2) \bar{\Gamma}_3 + P \rho_{102} \Gamma_2 + (\phi_{102}^2 + \rho_{102}^2) \bar{\Gamma}_2 + P \theta_{102} \Gamma_1 + \theta_{102}^2 \bar{\Gamma}_1.
 \end{aligned} \tag{B2}$$

The first three lines of this superpotential have already been discussed in the flavon alignment Sec. IV while the last four lines are needed to fix the phases of the various flavon VEVs. For instance, the messenger pair Γ_1 and $\bar{\Gamma}_1$ gives after integrating out the effective operator $1/\Lambda P \theta_{102}^3$ where in this case Λ stands for M_{Γ_1} multiplied by real order one couplings. This operator fixes the phase of $\langle \theta_{102} \rangle$ up to a discrete choice as discussed before.

We will not list here all of the effective operators because they have already appeared in our superpotential for the flavon alignment and they can also be read off from the diagrams in Fig. 3 after contracting the messenger propagators to points.

For the renormalizable couplings including the matter and Higgs fields we find the renormalizable superpotential (again dropping order one coefficients)

$$\begin{aligned}
 \mathcal{W}_d^{\text{ren}} = & T_3 \bar{H}_5 \bar{\Sigma}_3 + F \phi_3 \Sigma_3 + T_2 \phi_{23} \bar{Y}_1 + \bar{H}_{45} Y_1 \bar{\Xi}_1 \\
 & + F H_{24} \bar{\Xi}_1 + T_2 \phi_{102} \bar{Y}_2 + \bar{H}_5 Y_2 \bar{\Xi}_2 + \theta_{102} \bar{\Xi}_2 \bar{\Xi}_1 \\
 & + T_1 \phi_2 \bar{Y}_3 + \bar{H}_5 Y_3 \bar{\Xi}_3 + \theta_2 \bar{\Xi}_3 \bar{\Xi}_1,
 \end{aligned} \tag{B3}$$

$$\begin{aligned}
 \mathcal{W}_u^{\text{ren}} = & T_1 H_5 \Omega_3 + \xi_1 \Omega_2 \bar{\Omega}_3 + T_1 \xi_u \bar{\Omega}_2 + \Omega_2 \xi_u \bar{\Omega}_1 \\
 & + T_2 \Gamma_4 \bar{\Omega}_1 + \bar{\Gamma}_4 \xi_1^2 + T_2 H_5 \Omega_1 + T_3 \xi_1 \bar{\Omega}_1 \\
 & + T_3^2 H_5,
 \end{aligned} \tag{B4}$$

$$\begin{aligned}
 \mathcal{W}_\nu^{\text{ren}} = & \xi_1 N_1^2 + \xi_2 N_2^2 + F \phi_{23} \Sigma_1 + N_1 H_5 \bar{\Sigma}_1 \\
 & + F \phi_{102} \Sigma_2 + N_2 H_5 \bar{\Sigma}_2.
 \end{aligned} \tag{B5}$$

After integrating out the heavy messenger fields we end up with the nonrenormalizable operators as discussed in Sec. III; cf., also Figs. 4–6.

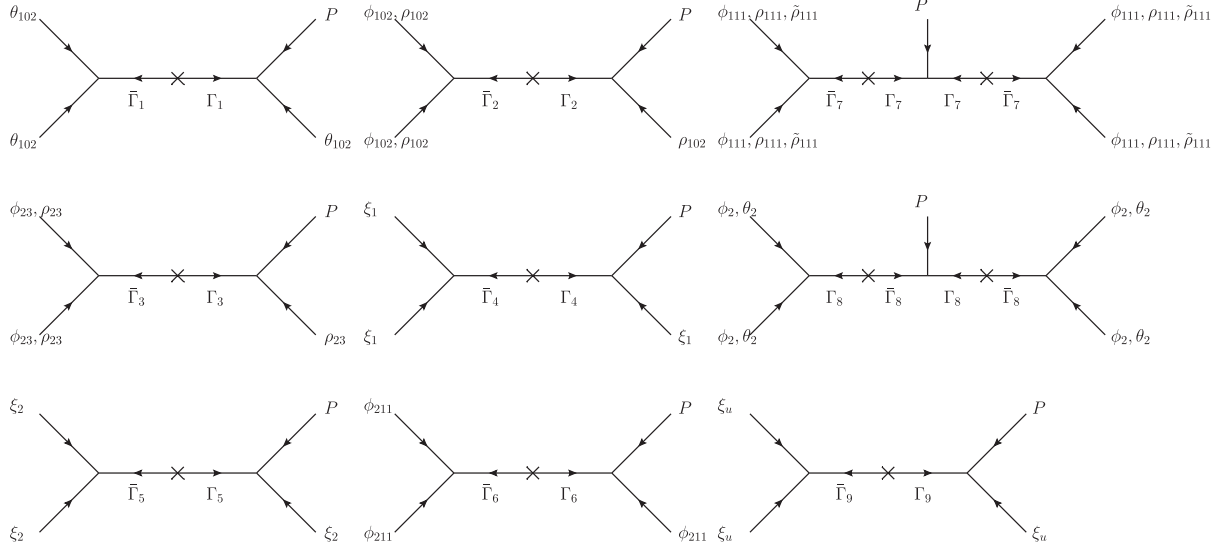


FIG. 3. The supergraphs before integrating out the messengers for the flavon sector (only diagrams are shown which give nonrenormalizable contributions).

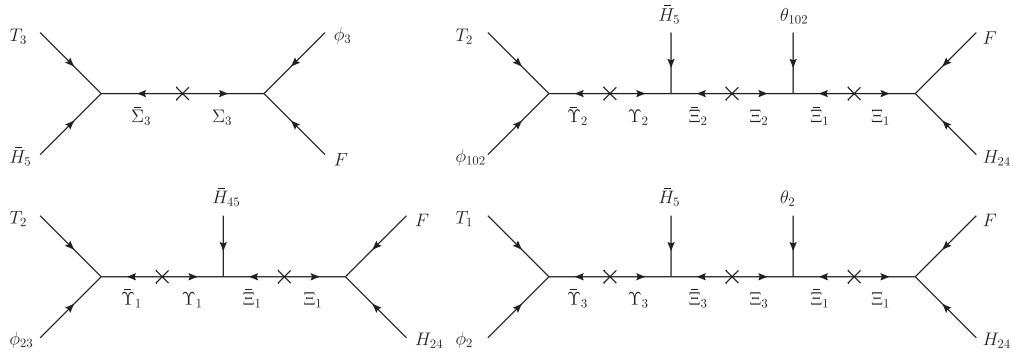


FIG. 4. The supergraphs before integrating out the messengers for the down-type quark and charged lepton sector.

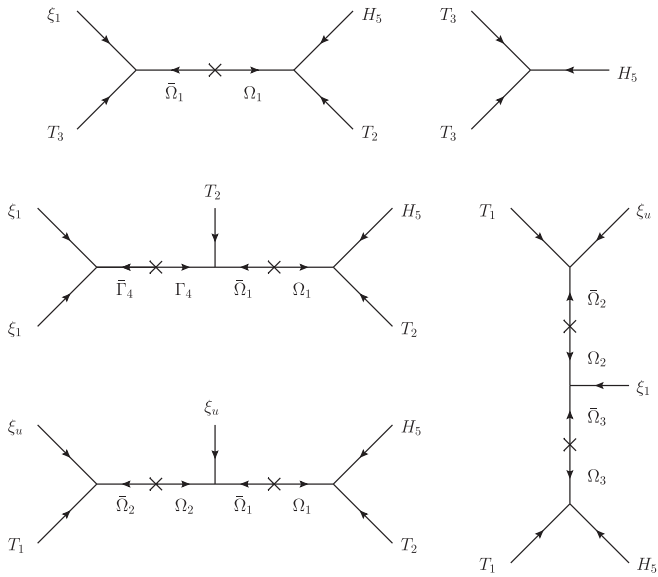


FIG. 5. The supergraphs before integrating out the messengers for the up-type quark sector.

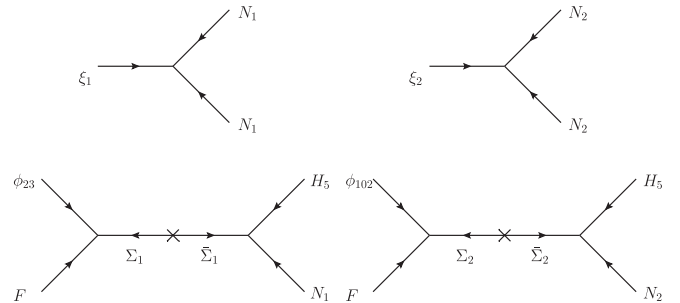


FIG. 6. The supergraphs before integrating out the messengers for the neutrino sector.

In addition to the renormalizable operators discussed so far there are six more operators allowed by the symmetries which are

$$\begin{aligned} \mathcal{W}_{\text{neg}}^{\text{ren}} = & T_1 \Gamma_9 \bar{\Omega}_1 + T_2 \Gamma_9 \bar{\Omega}_3 + \bar{\Xi}_1 \bar{\Xi}_3 \phi_2 + \Gamma_9 \Omega_1 \bar{\Omega}_2 \\ & + \Gamma_4 \bar{\Omega}_2 \Omega_3 + \Gamma_1 \bar{\Xi}_1 \bar{\Xi}_2. \end{aligned} \quad (\text{B6})$$

The first two operators contribute effectively to the $T_1 T_2 H_5 \xi_u^2$ operator already present and for the sake of simplicity we have not shown them in Fig. 5. The third operator generates the dimension six operator $FT_2 \bar{H}_{45} H_{24} \phi_2 \phi_{23}$ which gives a contribution to the 2–2 element of the down-type quark and charged lepton

Yukawa matrix. In fact the correction has the same phase and the same $SU(5)$ Clebsch-Gordan coefficient as the leading order coefficient so that we can safely neglect it. The last three operators finally give, after integrating out the heavy messengers, dimension seven and eight operators which give only small corrections (in our model we have discussed operators up to dimension six). The dimension seven operators, for instance, are induced by $\Gamma_9 \Omega_1 \bar{\Omega}_2$ which gives corrections to the 1–3 and 2–3 elements of the up-type quark Yukawa matrix which are very small compared to all other elements which are generated at maximum by a dimension five operator.

-
- [1] J. Beringer *et al.* (Particle Data Group), *Phys. Rev. D* **86**, 010001 (2012).
- [2] P. Adamson *et al.* (MINOS Collaboration), *Phys. Rev. Lett.* **107**, 181802 (2011).
- [3] Y. Abe *et al.* (Double Chooz Collaboration), *Phys. Rev. Lett.* **108**, 131801 (2012).
- [4] K. Abe *et al.* (T2K Collaboration), *Phys. Rev. Lett.* **107**, 041801 (2011).
- [5] F.P. An *et al.* (Daya-Bay Collaboration), *Phys. Rev. Lett.* **108**, 171803 (2012); Y. Wang, *What is ν ? INVISIBLES12 and Alexei Smirnov Fest* (Galileo Galilei Institute for Theoretical Physics, Italy, 2012), <http://indico.cern.ch/conferenceTimeTable.py?confId=195985>.
- [6] J.K. Ahn *et al.* (RENO Collaboration), *Phys. Rev. Lett.* **108**, 191802 (2012).
- [7] M. Ishitsuka, *Neutrino 2012* (Kyoto TERRSA, Japan, 2012), <http://kds.kek.jp/conferenceTimeTable.py?confId=9151>.
- [8] P.F. Harrison, D.H. Perkins, and W.G. Scott, *Phys. Lett. B* **530**, 167 (2002).
- [9] H.-J. He and F.-R. Yin, *Phys. Rev. D* **84**, 033009 (2011); Z.-Z. Xing, *Chinese Phys. C* **36**, 101 (2012); N. Qin and B.Q. Ma, *Phys. Lett. B* **702**, 143 (2011); Y.-j. Zheng and B.Q. Ma, *Eur. Phys. J. Plus* **127**, 7 (2012); S. Zhou, *Phys. Lett. B* **704**, 291 (2011); T. Araki, *Phys. Rev. D* **84**, 037301 (2011); N. Haba and R. Takahashi, *Phys. Lett. B* **702**, 388 (2011); D. Meloni, *J. High Energy Phys.* **10** (2011) 010; S. Morisi, K.M. Patel, and E. Peinado, *Phys. Rev. D* **84**, 053002 (2011); W. Chao and Y.-j. Zheng, *J. High Energy Phys.* **02** (2013) 044; H. Zhang and S. Zhou, *Phys. Lett. B* **704**, 296 (2011); X. Chu, M. Dhen, and T. Hambye, *J. High Energy Phys.* **11** (2011) 106; P.S. Bhupal Dev, R.N. Mohapatra, and M. Severson, *Phys. Rev. D* **84**, 053005 (2011); R. de Adelhart Toorop, F. Feruglio, and C. Hagedorn, *Phys. Lett. B* **703**, 447 (2011); S.F. King and C. Luhn, *J. High Energy Phys.* **09** (2011) 042; Q.-H. Cao, S. Khalil, E. Ma, and H. Okada, *Phys. Rev. D* **84**, 071302 (2011); S.-F. Ge, D.A. Dicus, and W.W. Repko, *Phys. Rev. Lett.* **108**, 041801 (2012); F. Bazzocchi, [arXiv:1108.2497](https://arxiv.org/abs/1108.2497); H.-J. He and X.-J. Xu, *Phys. Rev. D* **86**, 111301 (2012); S.F. King, *Phys. Lett. B* **718**, 136 (2012).
- [10] S. Antusch and V. Maurer, *Phys. Rev. D* **84**, 117301 (2011); S. Antusch, C. Gross, V. Maurer, and C. Sluka, *Nucl. Phys.* **B866**, 255 (2013).
- [11] D. Marzocca, S. T. Petcov, A. Romanino, and M. Spinrath, *J. High Energy Phys.* **11** (2011) 009.
- [12] S.F. King, C. Luhn, and A.J. Stuart, *Nucl. Phys.* **B867**, 203 (2013); C. Hagedorn, S.F. King, and C. Luhn, *Phys. Lett. B* **717**, 207 (2012); I.K. Cooper, S.F. King, and C. Luhn, *J. High Energy Phys.* **06** (2012) 130; I. de Medeiros Varzielas and G.G. Ross, *J. High Energy Phys.* **12** (2012) 041.
- [13] A. Meroni, S. T. Petcov, and M. Spinrath, *Phys. Rev. D* **86**, 113003 (2012).
- [14] N. Haba, A. Watanabe, and K. Yoshioka, *Phys. Rev. Lett.* **97**, 041601 (2006); X.-G. He and A. Zee, *Phys. Lett. B* **645**, 427 (2007); W. Grimus and L. Lavoura, *J. High Energy Phys.* **09** (2008) 106; H. Ishimori, Y. Shimizu, M. Tanimoto, and A. Watanabe, *Phys. Rev. D* **83**, 033004 (2011); Y. Shimizu, M. Tanimoto, and A. Watanabe, *Prog. Theor. Phys.* **126**, 81 (2011); X.-G. He and A. Zee, *Phys. Rev. D* **84**, 053004 (2011).
- [15] C.S. Lam, *Phys. Rev. D* **74**, 113004 (2006); C.H. Albright and W. Rodejohann, *Eur. Phys. J. C* **62**, 599 (2009); C.H. Albright, A. Dueck, and W. Rodejohann, *Eur. Phys. J. C* **70**, 1099 (2010).
- [16] S.F. King and C. Luhn, *J. High Energy Phys.* **09** (2011) 042; I.K. Cooper, S.F. King, and C. Luhn, *J. High Energy Phys.* **06** (2012) 130; C. Hagedorn, S.F. King, and C. Luhn, *Phys. Lett. B* **717**, 207 (2012).
- [17] S. Antusch, S.F. King, C. Luhn, and M. Spinrath, *Nucl. Phys.* **B856**, 328 (2012).
- [18] S.F. King, *Phys. Lett. B* **439**, 350 (1998); S.F. King, *Nucl. Phys.* **B562**, 57 (1999); S.F. King, *Nucl. Phys.* **B576**, 85 (2000); S.F. King, *J. High Energy Phys.* **09** (2002) 011; S. Antusch, S. Boudjemaa, and S.F. King, *J. High Energy Phys.* **09** (2010) 096.
- [19] S.F. King, *J. High Energy Phys.* **09** (2002) 011; S.F. King, *J. High Energy Phys.* **08** (2005) 105.
- [20] S.F. King, *Phys. Lett. B* **675**, 347 (2009).
- [21] K. Harigaya, M. Ibe, and T. T. Yanagida, *Phys. Rev. D* **86**, 013002 (2012).

- [22] S. Antusch, S.F. King, C. Luhn, and M. Spinrath, *Nucl. Phys.* **B850**, 477 (2011).
- [23] S.F. King and C. Luhn, *Rep. Prog. Phys.* **76**, 056201 (2013).
- [24] A detailed review and references can be found in G.C. Branco, R. G. Felipe, and F.R. Joaquim, *Rev. Mod. Phys.* **84**, 515 (2012).
- [25] G. G. Ross, L. Velasco-Sevilla, and O. Vives, *Nucl. Phys.* **B692**, 50 (2004).
- [26] S. F. King and M. Malinsky, *Phys. Lett. B* **645**, 351 (2007).
- [27] F. Feruglio, C. Hagedorn, and R. Ziegler, [arXiv:1211.5560](https://arxiv.org/abs/1211.5560); M. Holthausen, M. Lindner, and M. A. Schmidt, *J. High Energy Phys.* **04** (2013) 122.
- [28] H. Georgi and C. Jarlskog, *Phys. Lett.* **86B**, 297 (1979).
- [29] S. Antusch and S.F. King, *Phys. Lett. B* **631**, 42 (2005).
- [30] S. Antusch, S.F. King, and M. Malinsky, *Nucl. Phys.* **B820**, 32 (2009).
- [31] G.L. Fogli, E. Lisi, A. Marrone, D. Montanino, A. Palazzo, and A.M. Rotunno, *Phys. Rev. D* **86**, 013012 (2012).
- [32] H. Minakata, H. Nunokawa, W.J.C. Teves, and R. Zukanovich Funchal, *Phys. Rev. D* **71**, 013005 (2005); A. Bandyopadhyay, S. Choubey, S. Goswami, and S.T. Petcov, *Phys. Rev. D* **72**, 033013 (2005).
- [33] S. Antusch, S.F. King, M. Malinsky, and M. Spinrath, *Phys. Rev. D* **81**, 033008 (2010).
- [34] S. Antusch and M. Spinrath, *Phys. Rev. D* **79**, 095004 (2009).
- [35] S. Antusch and M. Spinrath, *Phys. Rev. D* **78**, 075020 (2008).
- [36] A. Juttner (FLAG Working Group), [arXiv:1109.1388](https://arxiv.org/abs/1109.1388).
- [37] G. Aad *et al.* (ATLAS Collaboration), *Phys. Lett. B* **716**, 1 (2012); S. Chatrchyan *et al.* (CMS Collaboration), *Phys. Lett. B* **716**, 30 (2012).
- [38] U. Ellwanger, C. Hugonie, and A.M. Teixeira, *Phys. Rep.* **496**, 1 (2010).
- [39] J.C. Callaghan and S.F. King, *J. High Energy Phys.* **04** (2013) 034.
- [40] S. Antusch, J. Kersten, M. Lindner, M. Ratz, and M. A. Schmidt, *J. High Energy Phys.* **03** (2005) 024.
- [41] K. Kowalska, S. Munir, L. Roszkowski, E.M. Sessolo, S. Trojanowski, and Y.-L. S. Tsai, [arXiv:1211.1693](https://arxiv.org/abs/1211.1693).
- [42] T. Cheng, J. Li, T. Li, and Q.-S. Yan, [arXiv:1304.3182](https://arxiv.org/abs/1304.3182); N.D. Christensen, T. Han, Z. Liu, and S. Su, [arXiv:1303.2113](https://arxiv.org/abs/1303.2113)
- [43] Z.-z. Xing, H. Zhang, and S. Zhou, *Phys. Rev. D* **77**, 113016 (2008).
- [44] K. Nakamura *et al.* (Particle Data Group), *J. Phys. G* **37**, 075021 (2010).
- [45] H. Leutwyler, *Nucl. Phys. B, Proc. Suppl.* **94**, 108 (2001).